European Journal of Medicinal Chemistry 47 (2012) 337–344

Contents lists available at SciVerse ScienceDirect

European Journal of Medicinal Chemistry

journal homepage: http://www.elsevier.com/locate/ejmech

Original article

6-alkylsalicylates are selective Tip60 inhibitors and target the acetyl-CoA binding site

Massimo Ghizzoni [a,1], Jiang Wu [b,1], Tielong Gao [b], Hidde J. Haisma [a], Frank J. Dekker [a,*], Y. George Zheng [b,**]

[a] Department of Pharmaceutical Gene Modulation, Groningen Research Institute of Pharmacy, University of Groningen A. Deusinglaan 1, 9713 AV, Groningen, The Netherlands
[b] Department of Chemistry, Georgia State University, Atlanta, GA 30303, USA

ARTICLE INFO

Article history:
Received 29 June 2011
Received in revised form
27 October 2011
Accepted 1 November 2011
Available online 10 November 2011

Keywords:
Histone acetylation
Epigenetics
Anacardic acid
Histone acetyltransferase (HAT)
Inhibitors

ABSTRACT

Histone acetyltransferases are important enzymes that regulate various cellular functions, such as epigenetic control of DNA transcription. Development of HAT inhibitors with high selectivity and potency will provide powerful mechanistic tools for the elucidation of the biological functions of HATs and may also have pharmacological value for potential new therapies. In this work, analogs of the known HAT inhibitor anacardic acid were synthesized and evaluated for inhibition of HAT activity. Biochemical assays revealed novel anacardic acid analogs that inhibited the human recombinant enzyme Tip60 selectively compared to PCAF and p300. Enzyme kinetics studies demonstrated that inhibition of Tip60 by one such novel anacardic acid derive, **20**, was essentially competitive with Ac-CoA and non-competitive with the histone substrate. In addition, these HAT inhibitors effectively inhibited acetyltransferase activity of nuclear extracts on the histone H3 and H4 at micromolar concentrations.

1. Introduction

The plant natural product anacardic acid (AA, 6-pentadecylsalicylic acid) is isolated from cashew nut shell liquid and is used in traditional medicine. [1] It exerts beneficial biological effects such as antitumor activity [2] and antioxidant activity. [3] AA was also shown to inhibit the activity of oxidative enzymes, such as tyrosinase, [4] cyclooxygenase, [5] and lipoxygenase. [6] Interestingly, AA and its derivatives were reported to modulate the enzymatic activity of histone acetyltransferases (HATs), such as p300 and p300/CBP-associated factor (PCAF), and to affect HAT-dependent gene transcription [7–13].

HATs are grouped into distinct families based on their sequence and structural homology [14,15]. The best studied families are the GNAT (GCN5-related N-acetyltransferase) family that includes PCAF and GCN5, the p300/CBP family that includes p300, and the MYST family that includes Tip60 (TAT-interacting protein 60) and MOF (maleless on the first). Acetylation of histones and other proteins by HATs regulates chromatin restructuring, [16] protein stability, [17] enzyme activity, [18] protein–protein interaction, [19] metabolism, [20,21] etc. On the chromatin template, generally, histone acetylation is connected to activation of gene transcription, whereas acetylation of transcription factors can either activate or inactive gene transcription [22]. Combinations of acetylation and other posttranslational modifications regulate gene transcription in response to extra- and intracellular stimuli. Moreover, accumulating evidence reveals that HAT activities are deregulated in many diseases, which highlights the pharmacologic importance of HATs as potential drug targets [23,24]. Acetylations of the nuclear factor κB (NF-κB) transcription factor as well as the histones play a crucial role in activation of this pathway [25]. Recent years have seen great efforts for designing and screening chemical HAT modulators [26–28]. The known HAT inhibitor AA has been shown to inhibit NF-κB mediated gene transcription, presumably by inhibition of the HAT p300 [29]. Furthermore, it has been shown that AA inhibits Tip60, which is one key member of the MYST family. AA blocks the Tip60-dependent activation of the ataxia telangiectasia mutated (ATM) protein kinase and the DNA-dependent protein kinase, catalytic subunit (DNA–PKcs) by DNA damage and sensitizes human tumor cells to the cytotoxic effects of ionizing radiation [8]. This indicates that HAT inhibition by small molecules provides a potential novel therapeutic approach for cancer and inflammatory diseases.

The molecular mechanism by which AA and its analogs inhibit HAT activity remains, however, poorly understood. It has been

* Corresponding author. Tel.: +31 503638030; fax: +31 50 3637953.
** Corresponding author. Tel.: +1 4044135491; fax: +1 4044135505.
E-mail addresses: f.j.dekker@rug.nl (F.J. Dekker), yzheng@gsu.edu (Y. George Zheng).
[1] These authors contributed equally to this work.

0223-5234/$ – see front matter © 2011 Elsevier Masson SAS. All rights reserved.
doi:10.1016/j.ejmech.2011.11.001

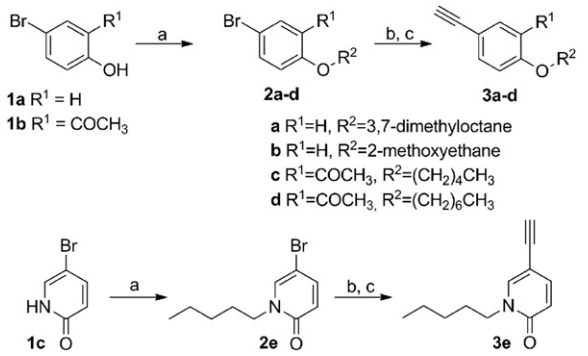

Scheme 1. Synthesis of acetylene building blocks for Sonogashira coupling. a) R-halide, K_2CO_3, DMF, b) TMS-acetylene, $PdCl_2(PPh_3)_2$, Et_2NH, CuI, PPh_3, CH_3CN, c) TBAF, THF.

suggested that the salicylate functionality of anacardic acid binds to the same pocket as the Ac-CoA pyrophosphate, [12] which suggest competitive binding in respect to Ac-CoA. In contrast, some studies suggested non-competitive inhibition for AA against Ac-CoA in p300 and PCAF assays, [7,30] which implicates a different inhibitory mechanism for p300 and PCAF.

Herein, we describe the design and synthesis of a series of AA analogs and the evaluation of their regulatory activity on the human recombinant HATs p300, PCAF, and Tip60 as well as cellular HAT activity. We aim to develop potent and selective inhibitors for recombinant HATs that also inhibit cellular HATs. Furthermore, we aim to gain a better understanding of the HAT inhibitory mechanism of AA analogs.

2. Chemistry

A compound collection was designed based on a versatile synthetic strategy, which includes two sonogashira couplings as key steps. This resulted in salicylate derivatives with a phenethyl substituent in the 6-position. This strategy allows including substituents with different polarities and sizes. The sonogashira couplings were performed under microwave irradiation, which provided fast conversion with moderate to high yields. Arylbromides were alkylated using alkylhalides to give the products **2a**–**2d** in high yields (>90%) (Scheme 1). Alkylation of **1c** provided the N-alkylated product **2e** as the main product in 55% yield. The O-alkylated product was isolated in minor amounts. The N-alkylated product **2e** showed a characteristic amide carbonyl signal in the IR spectrum, whereas this signal was absent in the corresponding O-alkylated product. Subsequently, the arylbromides were coupled to trimethylsilylacetylene by a Sonogashira coupling to yield the corresponding trimethylsilylalkynes in yields between 36 and 76%. The trimethylsilyl protective group was cleaved to give the corresponding alkynes **3a**–**3e**. Alkynes **3a**–**3e** were coupled to triflate **4** using Sonogashira couplings to provide compounds **5a**–**5e** in yields between 49 and 82% (Scheme 2). Hydrogenation of the alkynes using Pd/C under H_2 atmosphere and hydrolysis of the acetonide using KOH in THF provided compounds **6a-6c** and **6f**. Hydrogenation of **5c** using higher catalyst loading resulted in partial or complete reduction of the acetyl group to give either the ethyl (**6e**) or hydroxyethyl (**6d**) functionality. Furthermore, hydrogenation of alkyne **5e** resulted in reduction of the pentylpyridin-2(1H)-one functionality (**5e**) to give a pentylpiperidin-2-one functionality (**6g**). Compounds **9**, **12** and **15** (Scheme 2) present variations to the 6-alkyl substitution pattern of AA. These compounds were synthesized by Sonogashira couplings of alkynes on building blocks **7**, **10** and **13**. Products **8**, **11** and **14** were obtained in yields around 60%. These alkynes were hydrogenated using Pd/C under H_2 atmosphere. The methyl ester and methoxy functionality in **8** were simultaneously deprotected using BBr_3 and the methyl ester in **11** was hydrolyzed using KOH in THF. Hydrogenation of **14** provided the final product **15** in one step. Compound **16** (AA) to **26** have been published previously [12].

3. Pharmacology

3.1. Inhibitory potency of the AA analogs on three major HAT proteins

The potencies of **16** (AA) and its analogs to modulate the acetyltransferase activities of recombinant HATs were evaluated using human recombinant Tip60, PCAF and p300, which represent the three major HAT families in mammalian cells. Standard radioisotope-labeled histone acetyltransferase assays were carried out with ^{14}C-labeled Ac-CoA as the acetyl donor. Histone N-terminal peptides were used as the acetyl acceptor of the HAT reaction: H4-20 for p300 and Tip60 catalysis, and H3-20 for PCAF catalysis. The compounds shown in Scheme 1, 2 and in Table 1 were screened for inhibition of HAT activity. The compounds in Table 1 were published previously [12] The activities of the three HATs in the presence of 200 μM of each compound are collectively shown in Fig. 1. Clearly, the effect of the AA analogs on the enzymatic activity of the three HAT enzymes varies significantly from one to another, which offers the opportunity to derive structure–activity relationship (SAR).

The overall observation is that the **16** (AA) analogs show stronger inhibitory potency for Tip60 compared to p300 and PCAF, suggesting that the studied AA analogs have a general tendency for specific inhibition for the MYST HATs. In particular, compounds **6a**, **6c**, **16** (AA), **17**, **18**, **19** and **20** inhibited more than 76% of the Tip60

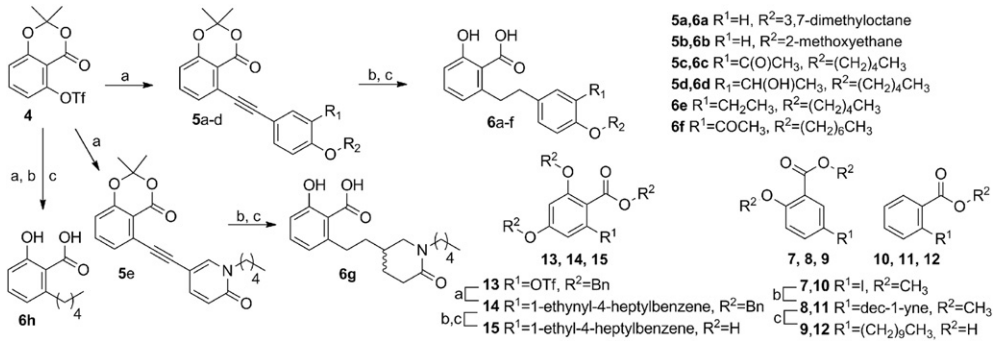

Scheme 2. Sonogashira coupling and subsequent hydrogenation and deprotection to give anacardic acid derivatives **6a**–**6h**. a) $PdCl_2(PPh_3)_2$, Et_2NH, CuI, PPh_3, CH_3CN, b) H_2, Pd/C, MeOH, c) KOH, THF.

Table 1
Previously published anacardic acid devatives that were applied in this study [12].

	R^1	R^2	R^3
16 (AA)	H	H	$-(CH_2)_{14}CH_3$
17	H	H	$-(CH_2)_9CH_3$
18	H	OH	$-(CH_2)_{14}CH_3$
19	H	OH	$-(CH_2)_9CH_3$
20	H	H	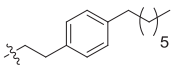
21	H	H	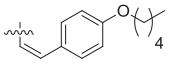
22	CH_3	H	$-(CH_2)_{14}CH_3$
23	H	H	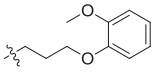
24	H	H	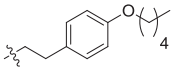
25	H	H	$-O(CH_2)_{13}CH_3$
26	H	H	$-OCH_2Ph$

activity at 200 μM, whereas their inhibitory effect on the activity of p300 and PCAF was little or very modest (≤35%). All these compounds have the conserved 6-substituted salicylate functionality, which highlights that this motif is critical for Tip60 inhibition. In contrast to compound **16** (AA) that inhibits the Tip60 activity almost completely, compound **22**, in which the carboxylate is replaced for a methyl ester, completely lost its inhibitory potency. Moreover, all the compounds with more than 70% inhibitory activity at 200 μM have an extended hydrophobic substituent in 6-position. In contrast, compounds with hydrophilic substituents, e.g. **6b** and **6d**, very weakly inhibit Tip60 at 200 μM. This indicates that hydrophobic substitution in the salicylate 6-position is indispensable for Tip60 inhibition. Compounds **16** (AA), **17** and **6h** show that aliphatic side chains with 10–15 carbon atoms (**16**, **17**) in the salicylate 6-position provide good inhibitory potency in contrast to aliphatic chains with 5 carbon atoms (**6h**). These data indicate that side chains that correspond to the length of a linear aliphatic chain with 10–15 carbon atoms provide good inhibitory potency. Also, it seems plausible that the first atom of the side chain adjacent to the salicylic ring needs to be a hydrophobic carbon, as replacement of this carbon by a hydrophilic oxygen greatly diminished inhibitory activity of the compounds. This is exemplified in compound **25** that contains an alpha-oxygen and shows only modest inhibitory activity.

In this study the potency of **16** (AA) deviates from studies previously published by others. For example, the IC_{50} of **16** (AA) was estimated be 8.5 μM for p300 and 5 μM for PCAF inhibition by Kundu et al. [7] In contrast, Souto et al. reported an IC_{50} between 50 and 100 uM for p300 [11]. In our previous characterization with a different assay, the IC_{50} of **16** (AA) is about 1000 μM for PCAF [12]. The last finding is well in line with our current finding that **16** (AA) inhibits about 20% of the HAT activity of p300 and PCAF at 200 μM. The reported differences demonstrate that the inhibitory potency of **16** (AA) depends strongly on the assay conditions and the enzyme source.

Of interest, some of the **16** (AA) analogs showed activation of the acetyltransferase activity of p300 and PCAF in contrast with the observed inhibitory effect on Tip60. Under the applied assay conditions, **21** and **24** enhance the PCAF activity significantly at a concentration of 200 μM. Our observations are not alone: the activation of HAT activity by several AA analogs was also observed previously [7,31,32,33]. However, the exact mechanism, the concentration dependence and time dependence of the activation remain to be investigated in order to validate small molecule HAT activation as a relevant phenomenon.

Among the effective Tip60 inhibitors, there are three salicylates with a phenethyl substitution in the 6-position, **6a**, **6c** and **20**. These inhibitors have calculated logD values at pH 7.4 of respectively 4.53, 3.07 and 4.19, which are lower than the calculated value 5.21 for **16** (AA) (calculated using MarvinSketch 5.4). The high logD value for AA is generally considered to be a disadvantage for its bioactivity [34] and therefore the inhibitors with the 6-phenethyl

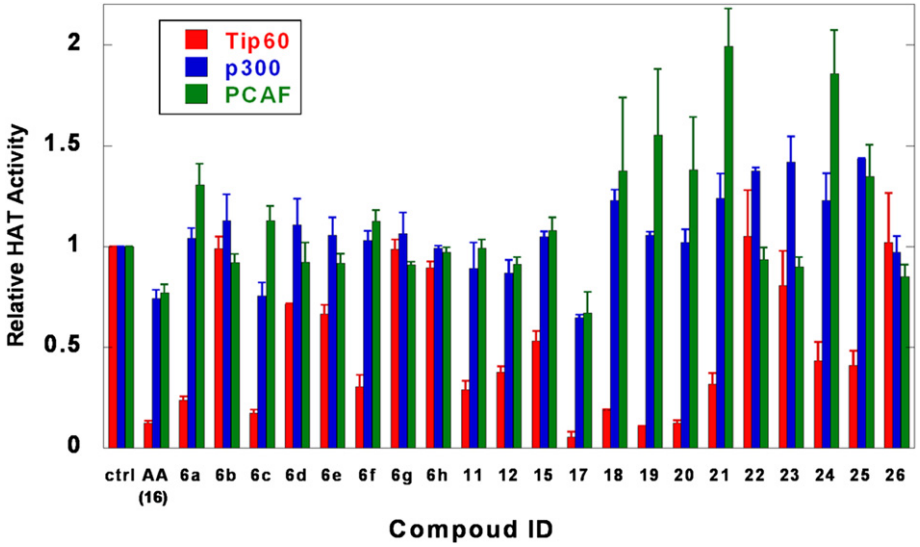

Fig. 1. The effect of **16** (AA) and its analogs on the HAT activity of the enzymes Tip60, p300, and PCAF. The inhibitors were applied at a concentration of 200 μM. For the Tip60 assay, the reaction mixture contained 100 nM Tip60, 10 μM Ac-CoA, 100 μM H4-20. For the p300 assay, the reaction mixture contained 5 nM p300, 10 μM Ac-CoA, and 100 μM H4-20. For the PCAF assay, the reaction mixture contained 5 nM PCAF, 10 μM Ac-CoA, and 100 μM H3-20.

Table 2
IC_{50} data of AA and **20** for the inhibition of HATs.

	IC_{50} of **16** (AA)	IC_{50} of **20**
Tip60	64 ± 15 μM	74 ± 20 μM
PCAF	>200 μM (40% inhibition)	>200 μM (3% inhibition)
p300	>200 μM (40% inhibition)	>200 μM (30% inhibition)
MOF	43 ± 2 μM	47 ± 14 μM

salicylate type can be considered improved leads for development of Tip60 inhibitors. Inhibitor **20** inhibited the Tip60 activity by 88% at 200 μM and had no observable inhibitory effect on p300 and PCAF, in contrast to AA that showed about 20% inhibition of these enzymes at 200 μM. We therefore selected this inhibitor for further evaluation in order to understand the potency and selectivity of this AA analog for HAT inhibition. We determined the IC_{50} value for inhibition of the HAT activity of Tip60 and MOF for **20** and compared that with **16** (AA). MOF is another MYST family HAT that is relevant in eukaryotic gene transcription. The IC_{50} was determined as the concentration of the inhibitor at which half of the enzyme activity was inhibited. The results are shown in Table 2. Under these experimental conditions, the IC_{50}'s of **16** (AA) and **20** are 64 μM and 74 μM for Tip60, and 43 μM and 47 μM for MOF. In contrast, IC_{50}'s of both **16** (AA) and **20** are higher than 200 μM for p300 and PCAF (the exact IC_{50} values cannot be determined due to compound insolubility at high concentrations). These data indicate that **16** (AA) and the other tested analogs tend to be specific inhibitors for the MYST family HATs. This is exemplified by **20**, which at 200 μM inhibited about 90% of Tip60 activity but had no inhibitory impact on p300 and PCAF (Fig. 1). The comparable inhibitory potency for the MYST family HATs Tip60 and MOF can be explained by the 67% sequence similarity in their catalytic region (Blast sequence alignment) [35].

3.2. Kinetic pattern of Tip60 inhibition by compound **20**

We carried out steady-state kinetic characterization of **20** for inhibition of Tip60 with respect to Ac-CoA and the H4 peptide to understand the mechanism by which the AA analogs inhibit the HAT activity of Tip60. The inhibition pattern was analyzed by measuring initial velocities of Tip60 at different concentrations of one substrate, a fixed concentration of the second substrate, and several selected concentrations of **20** (i.e. 0, 80, 120 μM). The Michaelis–Menten plots and the Lineweaver–Burk double reciprocal plots are shown in Fig. 2. To determine the inhibition pattern of compound **20**, the Michaelis–Menten data were fitted to the nonlinear non-competitive inhibition equation (1) [10]. In this equation, v is the measured initial reaction velocity, V is the maximal velocity (in the absence of inhibitor), [S] is the concentration of the varied substrate, K_m is the corresponding apparent Michaelis–Menten constant, [I] is the concentration of the inhibitor, and K_{is} and K_{ii} are the slope and intercept inhibition constants, respectively.

$$v = V[S]/[K_m(1 + [I]/K_{is}) + [S](1 + [I]/K_{ii})] \quad (1)$$

The Michaelis–Menten data were fit to equation (1) and yielded K_{is} of 54 μM and K_{ii} of 572 μM. Because K_{is} is 10-fold smaller than K_{ii}, it is concluded that the inhibition of Tip60 by **20** is essentially competitive with respect to Ac-CoA, binding to the same enzyme form. In the primary double reciprocal plot of E/V versus 1/[Ac-CoA] a series of straight lines intersect at a point very close to the

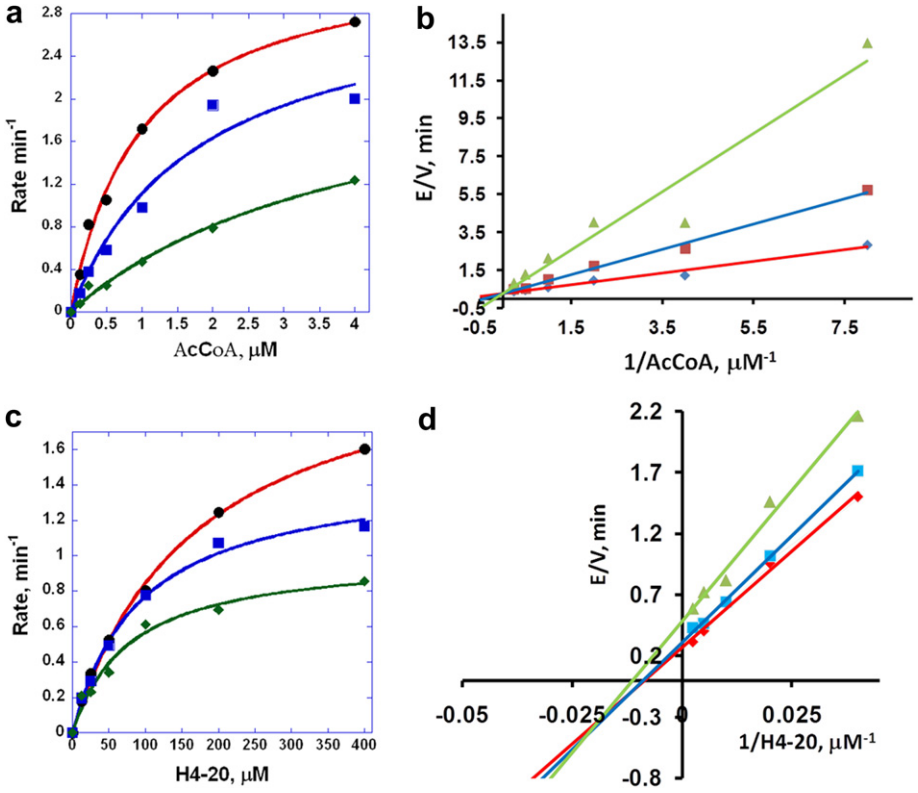

Fig. 2. Steady-state kinetic characterization of Tip60 inhibition by **20**. (a) and (b) Michaelis–Menten and Lineweaver–Burk plots showing relation of Tip60 activity versus Ac-CoA concentration at three selected concentrations of **20** (0 μM, red; 80 μM, blue; 120 μM, green). The reaction contained 50 nM Tip60 and 100 μM H4-20. (c) and (d) Michaelis–Menten and Lineweaver–Burk plots showing function of Tip60 activity versus H4-20 concentration at three selected concentrations of **20** (0 μM, red; 80 μM, blue; 120 μM, green). The reaction contained 25 nM Tip60 and 2 μM Ac-CoA. (For interpretation of the references to colour in this figure legend, the reader is referred to the web version of this article.)

ordinate, which further supports the competitive inhibition mode. The measurable K_{ii} may be an indication that **20** has additional weak binding site(s) in Tip60. On the other hand, the intersecting point in the double reciprocal plot of E/V versus 1/[H4-20] is clearly positioned to the left of the ordinate. The kinetic data fitting yielded K_{is} of >660 μM and K_{ii} of 78 μM. Therefore, **20** is non-competitive against the peptide substrate, preferentially binding to the enzyme form which is different from that the peptide binds to. The inhibitory pattern of **20** also offers insight into the kinetic mechanism of Tip60 catalysis. It suggests a likely ordered substrate binding pathway: Ac-CoA binds to Tip60 first and the peptide binds at a point downstream of Ac-CoA binding.

3.3. Docking study

To elucidate the structural basis of Tip60 inhibition by the AA analogs, we performed a docking study of **20** with the crystal structure of Tip60 HAT domain (PDB ID 2OU2). As displayed in Fig. 3, the 50 structural poses of the ligand were found to be located at four different regions in the Tip60 structure. In particular, half of the generated poses are located in the Ac-CoA binding pocket of Tip60 (i.e. region I). A further zoom-in examination reveals that in this site **20** or the adenine group of Ac-CoA interacts with several common amino acid residues of the Tip60, such as Ser364, Lys331, and Arg326. It is also interesting that the hydrophobic tail in molecule **20** shows a similar orientation as the long chain of Ac-CoA. These docking results suggest that **20** targets the active site of Tip60, which coincides well with the aforementioned steady-state kinetic analysis showing that inhibition by **20** is predominantly competitive with respect to Ac-CoA. The docking model provides a structural basis for future optimization to obtain more potent and selective AA analog inhibitors.

3.4. Inhibition of cellular HAT activity

The inhibition of HAT activity in nuclear extracts from HeLa cells or tissue samples from different brain regions from rats was studied using an ELISA assay. In this assay either the biotinylated histone H3

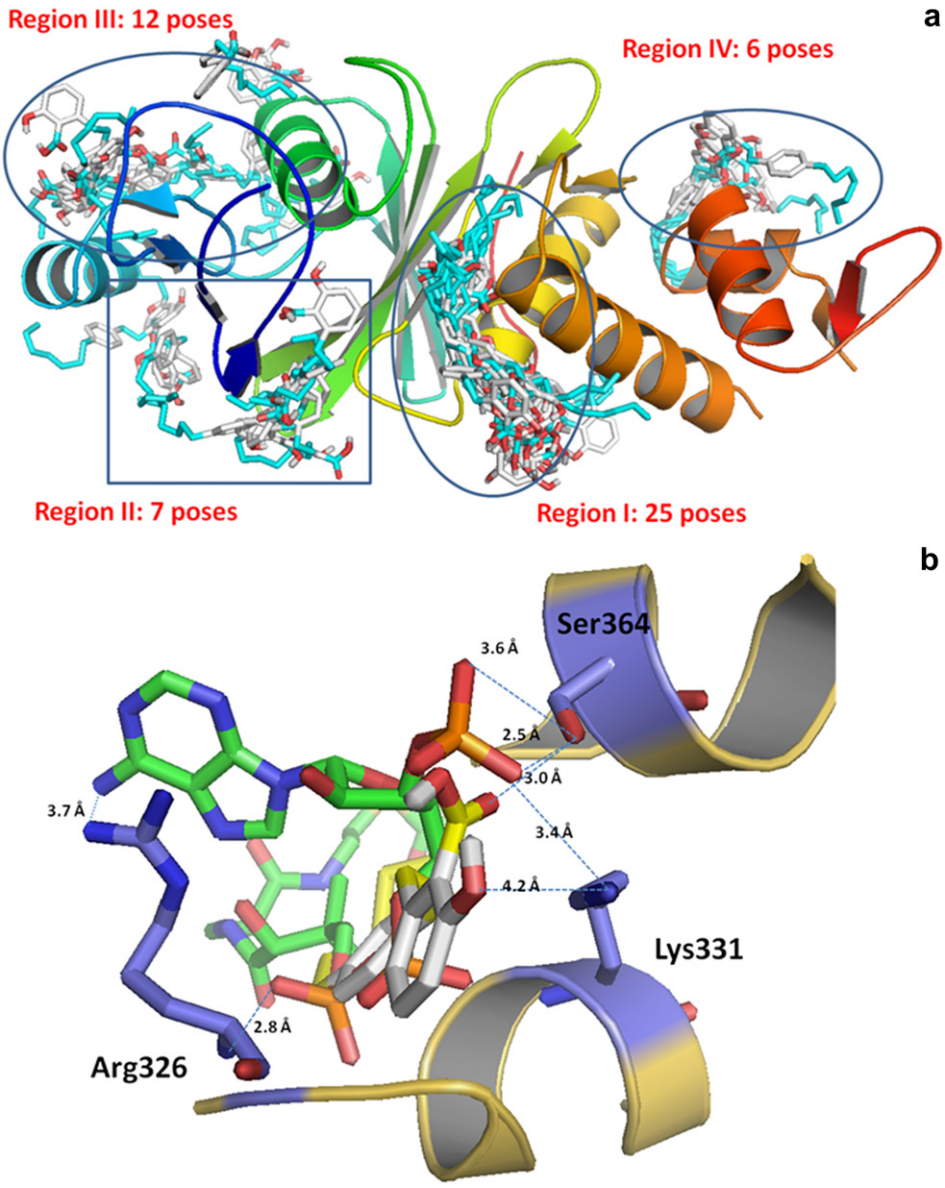

Fig. 3. Docking of **20** in the crystal structure (2OU2) of Tip60 HAT domain. (a) The spatial distribution of the 50 docking poses is clustered into four regions. (b) Ac-CoA and one pose in region I interact with some common residues of Tip60.

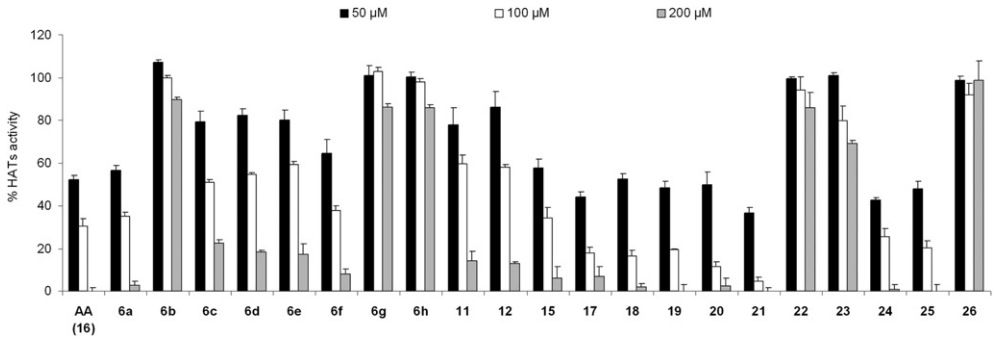

Fig. 4. Concentration dependent inhibition of HAT activity in HeLa nuclear extracts by AA analogs. Averages and standard deviations of triplicates are reported relative to the positive control in which no inhibitor was present and the negative control where no enzyme was present.

(aa 1–21) or histone H4 (aa 2–24) peptides were linked to a 96-well plate via streptavidin. The histone peptides were subjected to acetylation by using nuclear extracts as enzyme source and histone acetylation was detected using an anti-acetyl Lysine antibody. Most of the studied 6-alkylsalicylates show concentration dependent inhibition of histone H4 acetylation (Fig. 4). Compounds with a polar chain in the salicylate 6-position have a strongly reduced HAT inhibitory potency (**6b**, **6g**, **6h**, **23**, **26**). Also methylation of the salicylate carboxylate (**22**) is detrimental for the HAT inhibitory activity. An aliphatic substituent in the salicylate 6-position is beneficial for inhibition of HAT activity (**16** (AA), **17**, **18**, **19**). Interestingly, compound **21** that has been described previously to be a more potent inhibitor of histone acetylation than **16** (AA) in HEP G2 cells also showed high inhibitory activity on HeLa nuclear extracts [12].

It is of note that, the inhibition profile of the AA analogs on nuclear extract acetyltransferase activity correlates well with the assay on recombinant Tip60. For instance, the compounds that inhibited the cellular HAT activity more then 50% at 200 µM, e.g. **6a**, **6c**, **6f**, **11**, **12**, **16** (AA), **17**, **18**, **19**, **20**, **21**, **24**, and **25**, also inhibited the Tip60 HAT activity. On the other hand, most of the compounds that showed poor inhibition of HeLa nuclear extract activity, **6b**, **6g**, **6h**, **22**, **23**, and **26**, were also very poor inhibitors for the recombinant enzyme. The compounds **6d**, **6e** and **15** are exceptions because they seem to be more potent on HeLa nuclear extracts than for the recombinant Tip60. These observations could be explained by the presence of multiple HATs in nuclear extracts.

The inhibitory potency of the compound collection on histone H3 acetylation by HeLa nuclear extracts was investigated at 50 µM concentrations and compared to histone H4 acetylation (Supplementary data – Figure S1). Interestingly, a change in inhibitory potency was observed between histone H3 and histone H4. For example **16** (AA) and **17** show almost equal potency for both histones, whereas for example, **6a**, **6f**, **15**, **18** and **20**, are more potent for histone H3 compared to histone H4. The opposite is true for compounds like **21**, **24** and **25**. Given the complexity of HAT enzyme composition, distribution, and catalytic turnover rates of each HAT complex in the nucleus, it would be very difficult to interpret the differential impact of the AA analogs on H3 acetylation and H4 acetylation. However, the data shown here indicate that selective inhibitors towards histone H3 or H4 acetylation could be developed.

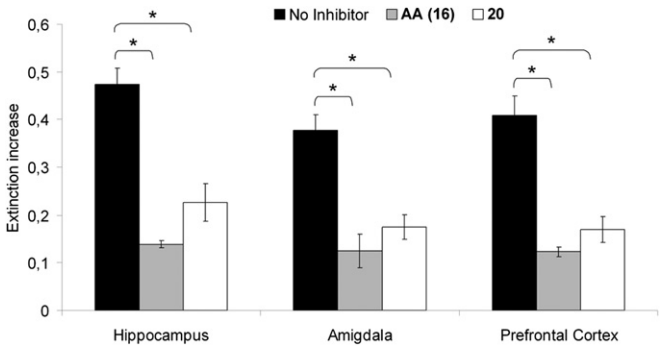

Fig. 5. Acetyltransferase activity of nuclear extract from tissue samples from different brain regions in mice. The acetyltransferase activity was determined using an ELISA assay with histone H3 as acetyl acceptor. The inhibitors **16** (AA) and **20** were applied in a concentration of 30 µM. Experiments were performed in triplicate for two different animals. The averages and standard deviations for the two animals are shown and blank values were subtracted. $^{*}p < 0.05$.

An assay on the HAT activity of nuclear extracts of brain tissue samples from rats showed no significant difference between HAT activity in brain tissue in different brain regions ($n = 3$, $p > 0.05$) (Fig. 5). Studies on two different animals showed no significant deviations between the animals ($n = 2$, $p > 0.05$). HAT inhibition studies with the inhibitors **16** (AA) and **20** demonstrated that both compounds inhibited the HAT activity of the nuclear extracts of different regions significantly ($p < 0.05$). Compound **20** showed slightly impaired inhibition compared to **16** (AA), which is statistically significant for the hippocampus ($p < 0.05$).

4. Conclusion

AA (**16**) analogs with various 2-phenylethane substituents in the salicylate 6-position were synthesized and tested for modulating enzymatic activities of three major types of mammalian HAT proteins. The recombinant enzyme inhibition assays demonstrated that inhibitors **18**, **19**, **20** and **21** are selective for Tip60 in comparison with PCAF and p300. Compounds that inhibited Tip60 showed in most cases also inhibition of HAT activity in HeLa nuclear extracts, which suggests that MYST type HATs play an important role in the HAT activity of the studied extracts. Inhibitor **20** was subjected to further investigation because its logD value is lower than AA, whereas it inhibitory potency on recombinant Tip60 as well as HeLa nuclear extracts is maintained. Enzyme kinetics showed that inhibition of Tip60 by **20** is competitive to Ac-CoA and non-competitive to histone H4, which supports the hypothesis that AA derivatives bind to the Ac-CoA binding pocket. Inhibitor **20** showed also equal potency to AA in nuclear extracts of tissue samples from different brain regions of rats, which indicates that **20** inhibits HAT activity from various sources.

5. Experimental section

5.1. Synthesis

See supplementary data.

5.2. Protein expression

His-tagged PCAF HAT domain (493-658) was expressed with the pET28a vector. His-tagged full length Tip60 was expressed with the pET21a(+) vector. Recombinant p300 HAT domain was a gift from Dr. Philip Cole. Human MOF (125-458) was expressed with the pET19 vector. All the protein expression was carried out with *E. coli* BL21(DE3). The His-tagged proteins were purified on Ni-NTA beads. Protein concentrations were determined using the Bradford assay. Proteins were flash frozen in a storage buffer containing 25 mM HEPES pH = 7.0, 500 mM NaCl, 10 mM DTT, 1 mM EDTA and 10% Glycerol, and stored at −80 °C.

5.3. Biochemical inhibition assays

Radioisotope-labeled acetyltransferase assays were carried out at 30 °C in a reaction volume of 30 μL. The reaction buffer contained 50 mM HEPES at pH 8.0, 0.1 mM EDTA, 50 μg/mL BSA, 1 mM dithiothreitol, 0.1% Triton-X100, and 2% DMSO. ^{14}C-labeled Ac-CoA (Perkin Elmer) was used as the acetyl donor. The peptide containing the N-terminal 20-amino acid sequence of histone H4 (i.e. H4-20) was used as substrate for p300 and Tip60, and the peptide containing the N-terminal 20-amino acid sequence of histone H3 (i.e. H3-20) was employed as substrate for PCAF. The HAT reaction was initiated with the HAT enzyme after the other components (Ac-CoA, peptide substrate, and the inhibitor) were equilibrated at 30 °C for 5 min. Rate measurements were based on initial conditions (generally less than 15% consumption of the limiting substrate). After the reaction, the mixture was loaded onto a Waterman P81 filter paper and then washed with 50 mM sodium bicarbonate (pH 9.0) for three times. The paper was air dried and the amount of radioactivity incorporated into the peptide substrate was quantified by liquid scintillation counting. In all the cases, background acetylation (in the absence of enzyme) was subtracted from the total signals. The IC_{50} was determined as the concentration of an inhibitor at which half of the enzyme activity was inhibited. For IC_{50} determination, a range of at least seven inhibitor concentrations varied at least 20-fold around the IC_{50} were tested. All the assays were performed at least twice, and duplicates generally agreed within 20%. The conditions for the IC_{50} measurement were; for the Tip60 assay, the reaction contained 10 nM Tip60, 1 μM Ac-CoA, 100 μM H4-20 and the reaction time was 7 min, for the PCAF assay, the reaction contained 1 nM PCAF, 1 μM Ac-CoA, 100 μM H3-20 and the reaction time was 3.5 min, for the p300 assay, the reaction contained 5 nM p300, 1 μM Ac-CoA, 100 μM H4-20 and the reaction time was 5 min, for the MOF assay, the reaction contained 1 nM MOF, 1 μM Ac-CoA, 100 μM H4-20 and the reaction time was 5 min. The conditions for the screening of the inhibitors are shown in the legend of Fig. 1.

5.4. Acetyltransferase assays with nuclear extracts

Nuclear extracts were prepared from HeLa cells or tissue samples for distinct brain regions using procedures described by Dignam et al. [36] The HAT activity in the nuclear extracts was determined using an ELISA assay in which either a biotinylated histone H3 peptide (aa 1 to 21, Anaspec − 61702) or a histone H4 peptide (aa 2-24, Millipore, 12-372) was immobilized using steptavidin-biotin linkage. The ELISA was performed as described previously [12]. The buffer for the enzymatic reaction contained 0.01% Triton X-100, 0.1 mM EDTA, 50 μg/mL BSA, 1 mM DTT and 50 mM HEPES pH 7.4. The nuclear extracts were standardized based on the protein concentration. The final protein concentration of the HeLa nuclear extract in the enzyme reaction was 2.5 μg/mL. For nuclear extracts of brain tissue samples the concentration was 40 μg/mL. The reaction time for the enzymatic reaction was 15 min. The brain tissue samples were obtained from Prof. Dr. B. Roozendaal, Neurosciences, UMCG, Groningen, The Netherlands. The samples were obtained from animal experiments that were approved by the animal experiment committee (Dier Experimenten Commissie, DEC) from this institute according to national regulations described in the 'law for animal experiments'.

5.5. Modeling

The PDB file of Tip60 structure (2OU2) was modified with Maestro 9.0.211 software to add hydrogens and delete the water and Ac-CoA molecules. The 3-dimensional structure of **20** was also constructed with Maestro 9.0.211. AutoDock Version 4.2 was then employed to generate PDBQT files for both the ligand and the macromolecule for docking. AutoGrid was used to generate a grid box covering the whole protein unit for docking processing. The Genetic Algorithm with 2,500,000 maximum numbers of evaluations and 50 generations for picking individuals was selected as the docking parameters. Structural analysis with PyMOL was performed following the docking process.

Acknowledgements

YGZ would like to acknowledge the partial financial support from AHA grant 09BGIA2220207 and NIH grant R01GM086717. We acknowledge Prof. Dr. B. Roozendaal, Neurosciences, University Medical Centre Groningen, The Netherlands for providing samples from rat brain tissue. We acknowledge A. Boltjes for his contribution to the synthesis of the anacardic acid analogs.

Appendix. Supplementary data

Supplementary data related to this article can be found online at doi:10.1016/j.ejmech.2011.11.001.

References

[1] J.T. Sullivan, C.S. Richards, H.A. Lloyd, G. Krishna, Anacardic acid: molluscicide in cashew nut shell liquid, Planta Med. 44 (1982) 175–177.
[2] A.I. Rea, J.M. Schmidt, W.N. Setzer, S. Sibanda, C. Taylor, E.T. Gwebu, Cytotoxic activity of *Ozoroa insignis* from Zimbabwe, Fitoterapia 74 (2003) 732–735.
[3] M.T. Trevisan, B. Pfundstein, R. Haubner, G. Wurtele, B. Spiegelhalder, H. Bartsch, R.W. Owen, Characterization of alkyl phenols in cashew (*Anacardium occidentale*) products and assay of their antioxidant capacity, Food Chem. Toxicol. 44 (2006) 188–197.
[4] I. Kubo, I. Kinst-Hori, Y. Yokokawa, Tyrosinase inhibitors from *Anacardium occidentale* fruits, J. Nat. Prod. 57 (1994) 545–551.
[5] R. Paramashivappa, P. Phani Kumar, P.V. Subba Rao, A. Srinivasa Rao, Design, synthesis and biological evaluation of benzimidazole/benzothiazole and benzoxazole derivatives as cyclooxygenase inhibitors, Bioorg. Med. Chem. Lett. 13 (2003) 657–660.
[6] T.J. Ha, I. Kubo, Lipoxygenase inhibitory activity of anacardic acids, J. Agric. Food Chem. 53 (2005) 4350–4354.
[7] K. Balasubramanyam, V. Swaminathan, A. Ranganathan, T.K. Kundu, Small molecule modulators of histone acetyltransferase p300, J. Biol. Chem. 278 (2003) 19134–19140.
[8] Y. Sun, X. Jiang, S. Chen, B.D. Price, Inhibition of histone acetyltransferase activity by anacardic acid sensitizes tumor cells to ionizing radiation, FEBS Lett. 580 (2006) 4353–4356.
[9] L. Cui, J. Miao, T. Furuya, Q. Fan, X. Li, P.K. Rathod, X. Su, L. Cui, Histone acetyltransferase inhibitor anacardic acid causes changes in global expression during in vitro *plasmodium falciparum* development, Eukaryotic. Cell 7 (2008) 1200–1210.
[10] J. Wu, N. Xie, Z. Wu, Y. Zhang, Y.G. Zheng, Bisubstrate inhibitors of the MYST HATs Esa1 and Tip60, Bioorg. Med. Chem. 17 (2009) 1381–1386.
[11] J.A. Souto, M. Conte, R. Alvarez, A. Nebbioso, V. Carafa, L. Altucci, A.R. de Lera, Synthesis of benzamides related to anacardic acid and their histone acetyltransferase (HAT) inhibitory activities, ChemMedChem. 3 (2008) 1435–1442.
[12] M. Ghizzoni, A. Boltjes, C. Graaf, H.J. Haisma, F.J. Dekker, Improved inhibition of the histone acetyltransferase PCAF by an anacardic acid derivative, Bioorg. Med. Chem. 18 (2010) 5826–5834.

[13] E.D. Eliseeva, V. Valkov, M. Jung, M.O. Jung, Characterization of novel inhibitors of histone acetyltransferases, Mol. Cancer Ther. 6 (2007) 2391.
[14] M.W. Vetting, L.P. S de Carvalho, M. Yu, S.S. Hegde, S. Magnet, S.L. Roderick, J.S. Blanchard, Structure and functions of the GNAT superfamily of acetyltransferases, Arch. Biochem. Biophys. 433 (2005) 212–226.
[15] K.K. Lee, J.L. Workman, Histone acetyltransferase complexes: one size doesn't fit all, Nat. Rev. Mol. Cell Biol. 8 (2007) 284–295.
[16] M. Shogren-Knaak, H. Ishii, J.M. Sun, M.J. Pazin, J.R. Davie, C.L. Peterson, Histone H4-K16 acetylation controls chromatin structure and protein interactions, Science 311 (2006) 844–847.
[17] F. Faiola, X. Liu, S. Lo, S. Pan, K. Zhang, E. Lymar, A. Farina, E. Martinez, Dual regulation of c-Myc by p300 via acetylation-dependent control of Myc protein turnover and coactivation of Myc-induced transcription, Mol. Cell. Biol. 25 (2005) 10220–10234.
[18] S. Daujat, U.M. Bauer, V. Shah, B. Turner, S. Berger, T. Kouzarides, Crosstalk between CARM1 methylation and CBP acetylation on histone H3, Curr. Biol. 12 (2002) 2090–2097.
[19] X.J. Yang, Lysine acetylation and the bromodomain: a new partnership for signaling, Bioessays 26 (2004) 1076–1087.
[20] Q. Wang, Y. Zhang, C. Yang, H. Xiong, Y. Lin, J. Yao, H. Li, L. Xie, W. Zhao, Y. Yao, Z.B. Ning, R. Zeng, Y. Xiong, K.L. Guan, S. Zhao, G.P. Zhao, Acetylation of metabolic enzymes coordinates carbon source utilization and metabolic flux, Science 327 (2010) 1004–1007.
[21] S. Zhao, W. Xu, W. Jiang, W. Yu, Y. Lin, T. Zhang, J. Yao, L. Zhou, Y. Zeng, H. Li, Y. Li, J. Shi, W. An, S.M. Hancock, F. He, L. Qin, J. Chin, P. Yang, X. Chen, Q. Lei, Y. Xiong, K.L. Guan, Regulation of cellular metabolism by protein lysine acetylation, Science 327 (2010) 1000–1004.
[22] F.J. Dekker, H.J. Haisma, Histone acetyl transferases as emerging drug targets, Drug Discov. Today 14 (2009) 942–948.
[23] X.J. Yang, The diverse superfamily of lysine acetyltransferases and their roles in leukemia and other diseases, Nucleic Acids Res. 32 (2004) 959–976.
[24] D.M. Heery, P.M. Fischer, Pharmacological targeting of lysine acetyltransferases in human disease: a progress report, Drug Discov. Today 12 (2007) 88–99.
[25] M. Ghizzoni, H.J. Haisma, H. Maarsingh, F.J. Dekker, Histone acetyltransferases are crucial regulators in NF-kappaB mediated inflammation, Drug Discov. Today 16 (2011) 504–511.
[26] T. Suzuki, N. Miyata, Epigenetic control using natural products and synthetic molecules, Curr. Med. Chem. 13 (2006) 935–958.
[27] M. Biel, V. Wascholowski, A. Giannis, Epigenetics – an epicenter of gene regulation: histones and histone-modifyng enzymes, Angew. Chem. Int. Ed. 44 (2005) 3186–3216.
[28] Y.G. Zheng, J. Wu, Z. Chen, M. Goodman, Chemical regulation of epigenetic modifications: opportunities for new cancer therapy, Med. Res. Rev. 28 (2008) 645–687.
[29] B. Sung, M.K. Pandey, K.S. Ahn, T. Yi, M.M. Chaturvedi, M. Liu, B.B. Aggarwal, Anacardic acid (6-nonadecyl salicylic acid), an inhibitor of histone acetyltransferase, suppresses expression of nuclear factor-kappaB-regulated gene products involved in cell survival, proliferation, invasion, and inflammation through inhibition of the inhibitory subunit of nuclear factor-kappaBalpha kinase, leading to potentiation of apoptosis, Blood 111 (2008) 4880–4891.
[30] L. Cui, J. Miao, T. Furuya, Q. Fan, X. Li, P.K. Rathod, X.Z. Su, L. Cui, Histone acetyltransferase inhibitor anacardic acid causes changes in global gene expression during in vitro Plasmodium falciparum development, Eukaryot, Cell 7 (2008) 1200–1210.
[31] G. Sbardella, S. Castellano, C. Vicidomini, D. Rotili, A. Nebbioso, M. Miceli, L. Altucci, A. Mai, Identification of long chain alkylidenemalonates as novel small molecule modulators of histone acetyltransferases, Bioorg. Med. Chem. Lett. 18 (2008) 2788–2792.
[32] J.A. Souto, R. Benedetti, K. Otto, M. Miceli, R. Alvarez, L. Altucci, A.R. de Lera, New anacardic acid-inspired benzamides: histone lysine acetyltransferase activators, ChemMedChem. 5 (2010) 1530–1540.
[33] K. Mantelingu, B.A. Reddy, V. Swaminathan, A.H. Kishore, N.B. Siddappa, G.V. Kumar, G. Nagashankar, N. Natesh, S. Roy, P.P. Sadhale, U. Ranga, C. Narayana, T.K. Kundu, Specific inhibition of p300-HAT alters global gene expression and represses HIV replication, Chem. Biol. 14 (2007) 645–657.
[34] A. Böcker, P.R. Bonneau, O. Hucke, A. Jakalian, P.J. Edwards, Development of specific "Drug-Like Property" Rules for carboxylate-containing Oral drug Candidates, ChemMedChem 12 (2010) 2102–2113.
[35] S.F. Altschul, T.L. Madden, A.A. Schaffer, J. Zhang, Z. Zhang, W. Miller, D.J. Lipman, Gapped BLAST and PSI-BLAST: a new generation of protein database search programs, Nucleic Acids Res. 25 (1997) 3389–3402.
[36] J.D. Dignam, R.M. Lebovitz, R.G. Roeder, Accurate transcription initiation by RNA polymerase II in a soluble extract from isolated mammalian nuclei, Nucleic Acids Res. 11 (1983) 1475–1489.